doi:10.1016/j.jmb.2006.04.056 J. Mol. Biol. (2006) 360, 45–55

JMB

Available online at www.sciencedirect.com

SCIENCE DIRECT®

ELSEVIER

Membrane-transferring Sequences of the HIV-1 Gp41 Ectodomain Assemble into an Immunogenic Complex

Maier Lorizate[1], María J. Gómara[1], Beatriz G. de la Torre[2] David Andreu[2] and José L. Nieva[1]*

[1]*Biophysics Unit (CSIC-UPV/EHU) and Biochemistry Department, University of the Basque Country, P.O. Box 644, 48080 Bilbao, Spain*

[2]*Proteomics Unit, Pompeu Fabra University, Dr. Aiguader 80, 08003 Barcelona, Spain*

**Corresponding author*

The membrane-proximal stem region of gp41 has been postulated to host the two conserved membrane-transferring domains that promote HIV-1 fusion: the amino-terminal fusion peptide (FP) and the highly aromatic pre-transmembrane sequence. Our results confirm that the hydrophobic FP and membrane-proximal sequences come into contact and form structurally defined complexes. These complexes are immunogenic and evoke responses in rabbits that compete with the recognition of native functional gp41 by the 2F5 monoclonal antibody. We conclude that co-assembly of the FP and the pre-transmembrane sequences might exert a constraint that helps maintain a gp41 stem region pre-fusion structure.

Keywords: HIV-1; gp41; HIV-1 fusion peptide; gp41 pre-transmembrane; 2F5 antibody

Introduction

Envelope protein-induced fusion of the viral and the plasma membranes enables the human immunodeficiency virus type-1 (HIV-1) to enter into the $CD4^+$ target cell.[1–4] The fusogenic activity of the gp120/41 envelope glycoprotein is triggered by the sequential binding of the surface gp120 subunit to CD4 and to human chemokine receptors.[5,6] Subsequently, and in conjunction with the formation of a low-energy six-helix bundle structure, the transmembrane gp41 subunit promotes the merging of the lipid bilayers.[7–11] Mutational analyses indicate that the activity of gp41 is dependent on two hydrophobic ectodomain sequences: the free amino-terminal fusion peptide (FP),[12,13] which is not exposed to the solvent in the metastable structure primed for fusion,[2,3] and the highly aromatic pre-transmembrane region (preTM).[14]

Given the hydrophobic character of FP and preTM, it has been postulated that during the process of fusion these sequences insert into the target cell and the virion membranes, respectively.[15] When compared with other sequences that insert into membranes, such as signal peptides or transmembrane domains, the FP and preTM sequences display an unusually high degree of conservation.[14–17] Although atomic structures of gp41 states prior to the six-helix bundle form are not elucidated, predictive work[18] and epitope-mapping[19] suggest that both membrane-transferring regions might be located at the same end of the ectodomain, proximal to the virion envelope, in the native state. Here, we have used the 2F5 monoclonal antibody (Mab2F5),[20,21] which recognizes pre-fusion stem structures,[22] to test the hypothesis that the amino-terminal of gp41 and the membrane-proximal hydrophobic regions assemble into a defined complex.

In support of this hypothesis, the FP increased recognition of 2F5 linear epitope, a fact that correlated with establishment of interactions mediated specifically by the canonical FLG tripeptide duplication.[16] The FP also stabilized distinct conformations and promoted self-oligomerization of a sequence that combined the 2F5 linear epitope and the preTM domain. Consistent with a native-like epitope presentation, the complexes formed could elicit in rabbits immunoglobulins that competed efficiently for Mab2F5 epitope recognition. We conclude that FP may impart a native-like orientation/conformation onto the membrane-proximal gp41 residues. Our findings may help understanding pre-fusion gp41 structure–function relationships, and guide future

Abbreviations used: HIV-1, human immunodeficiency virus type-1; FP, fusion peptide; preTM, pre-transmembrane region; HFIP, 1,1,1,3,3,3-hexafluoro-2-propanol; Mab, monoclonal antibody.

E-mail address of the corresponding author: gbpniesj@lg.ehu.es

strategies to modulate the immunogenicity of gp41 epitope mimics.

Results

The gp41 ectodomain contains two sequences that show a significant tendency to partitioning into membrane interfaces: the amino-terminal FP and the preTM[15,23] (Figure 1(a)). The Mab2F5 antibody recognizes the linear epitope 656*NEQELLEL*DKWASLWN671[24,25] that connects the gp41 carboxy-helical C-terminal domain (in italics) with the highly aromatic preTM sequence 664DKWASLWNWFNITNWLWYIK683. The epitope face bound by the 2F5 antigen-binding fragment (Fab2F5) is charged, while the non-bound side is hydrophobic.[22] This arrangement implies that the hydrophobic surface of the unbound 2F5 epitope is occluded by other portions of gp41 ectodomain. As a working hypothesis, we proposed that the hydrophobic FP might be occluding this surface (Figure 1(b)). In order to identify the sequences in the amino-terminal region of gp41 that are capable of orientating the 2F5 epitope, Mab2F5 epitope-binding enhancement was mapped by mixing a representative 2F5ep peptide (Table 1) with overlapping 15-mer peptides that extended over the 497–559 region of gp160 (see diagrams in Figure 1, green areas). ELISA results displayed in Figure 2(a) show that the VGIGAMFLGFLGAAG peptide was the most effective in enhancing Mab2F5 binding, in accordance with the idea that the conserved FP domain was sufficiently hydrophobic to orientate the 2F5 epitope immobilized on plaques.

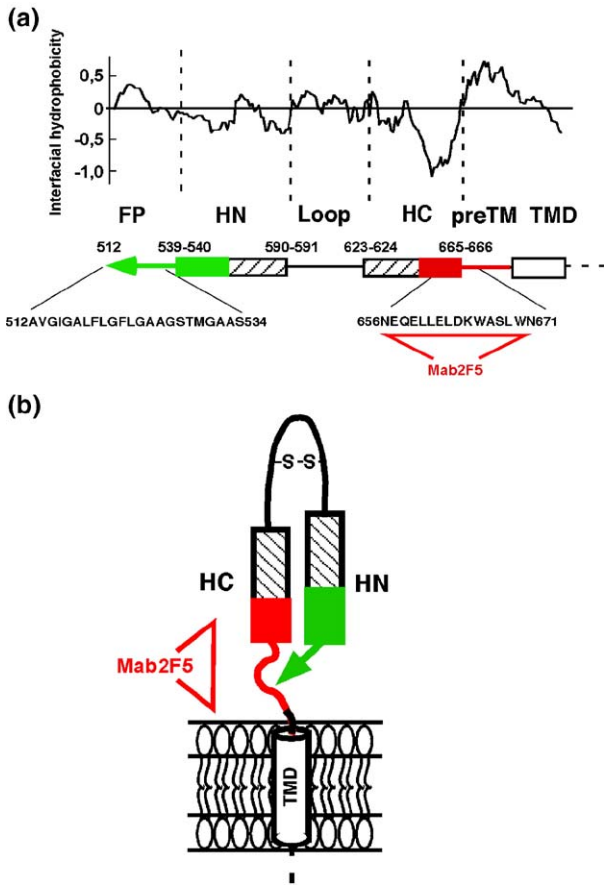

Figure 1. (a) A representation of the HIV-1 gp41 ectodomain and location of membrane-transferring sequences. The interfacial hydrophobicity plot represents, for a window of 11 amino residues, mean values of free energies of transfer from membrane interfaces to water (i.e. positive values denote a tendency for partitioning into the membrane interface). Free energy values for individual residues were obtained from the Wimley–White scale.[49] The regions designated below include: FP, fusion peptide; HN, amino helix; HC, carboxy helix; preTM, pretransmembrane; TMD transmembrane domain. Amino acid sequences are based on the BH10 isolate (Gen Bank accession no. M15654). (b) model of gp41 anchored to the viral membrane. The HN and HC cylinders corresponding to the potential helical domains are depicted in the same scale as the previous panel. The green and red areas denote the regions spanned by the peptide library used in ELISA experiments (Figure 2).

Membrane-proximal sequences containing the 2F5 ELDKWA core-epitope (see diagrams in Figure 1, red areas) were further scanned to determine whether they might increase the reactivity in the presence of the genuine FP 23-mer (Table 1). The greatest enhancement was observed with the 2F5ep-like EQELLELDKWASLWN sequence (Figure 2(b)). However, no improvement in FP-induced binding occurred when the ELDKWA hexapeptide was immobilized on the plaques, suggesting that the effect was sustained by residues outside the core-epitope that increase Mab2F5 affinity.[25]

These results indicated that the gp41 FP and the membrane-proximal sequences may co-assemble (Figure 1(b)), although any sequence that might contribute sufficient hydrophobicity could be expected to orientate the 2F5ep in plaques. In order to determine whether there was specific requirement for the FP-2F5ep complex to form, over and above the non-specific capacity of the hydrophobic elements to induce aggregation, we first analyzed the interactions between water-soluble derivatives by circular dichroism (CD, Figures 3 and 4) and subsequently confirmed the existence of structure-specific effects for Mab2F5-2F5ep binding in solution (Figure 5).

FPK3, which incorporated three Lys at its C terminus[26] (Table 1), and 2F5ep displayed CD spectra that were characteristic of water-soluble monomeric species with no predominant secondary structure in the 10–300 μM range (not shown). However, a comparison of the experimental spectra (continuous lines) and those calculated for the addition of non-interacting peptide signals (dotted lines), revealed a conformational rearrangement in the FPK3:2F5ep mixtures (Figure 3). The experimental spectra obtained in HFIP-free buffer displayed a weaker negative band, a shoulder shifted towards lower wavelengths, and more positive absorption at 190 nm. In the presence of 5% and 12.5% of the structure-promoting 1,1,1,3,3,3-hexafluoro-2-

Table 1. Peptide sequences used in this study

Name	Sequence	Gp160 numbering
FP	AVGIGALFLGFLGAAGSTMGARS	512–534
FPK3	AVGIGALFLGFLGAAGSTMGARSKKK	512–534-KKK
2F5ep	NEQELLELDKWASLWN	656–671
preTM	DKWASLWNWFNITNWLWYIK	664–683
2F5preTM	NEQELLELDKWASLWNWFNITNWLWYIK	656–683

Numbering is based on the BH10 isolate (GenBank accession no. **M15654**).

propanol (HFIP) similar experimental spectra were measured, with positive bands centered at 195 nm and negative bands at ca 208 nm and 222 nm, characteristic of complexes with a high content of α-helix. The shift of the positive red band together with a $[\theta]_{222}/[\theta]_{208}$ ellipticity ratio >1 (Table 2) supports the existence of helix–helix interactions such as those described for heterodimeric coiled-coils[27,28] and/or transmembrane helical bundles.[29] In contrast, the spectra calculated for non-interacting peptides displayed prominent negative peaks around 200 nm, which shifted and became progressively more intense. In 25% HFIP, the experimental and calculated spectra coincided. The positive peak that reverted to 190 nm, together with the $[\theta]_{222}/[\theta]_{208}$ ratios <1, are consistent with the disruption of the helix–helix interactions (Table 2).[28] Thus, the CD signals derived from the mixtures suggested the presence of heterodimeric interactions between chains, consistent with the co-assemble FPK3 and 2F5ep into a complex.

Shorter water-soluble derivatives were then analyzed to define the FP sequence that sustained the spectral differences observed in the FPK3:2F5ep

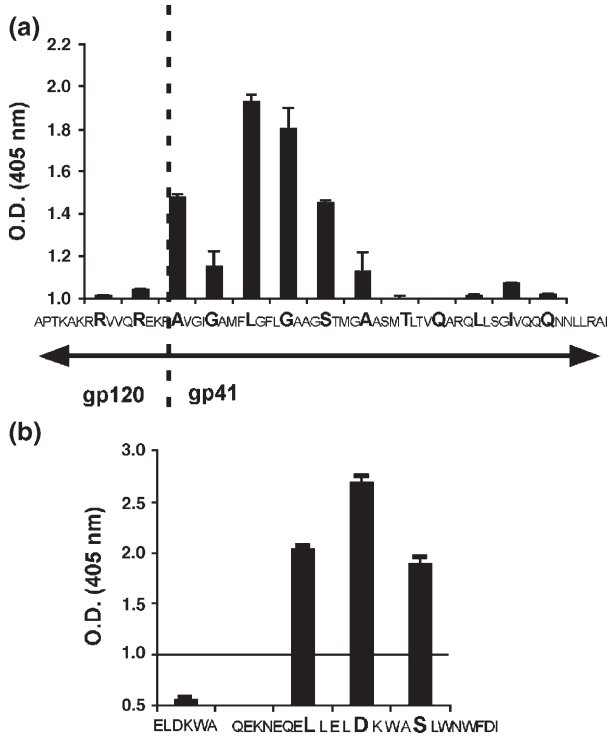

Figure 2. Mapping of gp41 regions that enhance Mab2F5 reactivity as detected in peptide-based ELISAs. (a) Effect of the gp41 amino-terminal region on recognition of 2F5ep by Mab2F5 (0.075 μg/ml). The 15-mer consecutive peptides (overlapping by 11 amino acid residues) which span the gp160 497–559 region (displayed as green areas in Figure 1) were mixed with 2F5ep at equimolar ratios in DMSO, and immobilized in plaques (each at final concentration of 1.4 μM). The central residue within the sliding window is indicated by the bold characters. In each experiment, the increase in absorbance was normalized to the level detected in parallel control samples using 2F5ep alone (1.0 absorbance). The signal from the amino-terminal sequence alone was negligible in these assays (not shown). The plotted values correspond to the means±standard deviation of three independent experiments. (b) Effect of the FP 23-mer on Mab2F5 recognition of consecutive 15-mer peptides spanning the gp41 membrane proximal region (red areas in Figure 1). To ensure recognition, the ELDKWA control hexapeptide was applied to the plaques at a higher concentration (26 μM) and mixed previously either at an equimolar ratio or with 1.4 μM FP (not shown). The effect of FP was comparable in both cases.

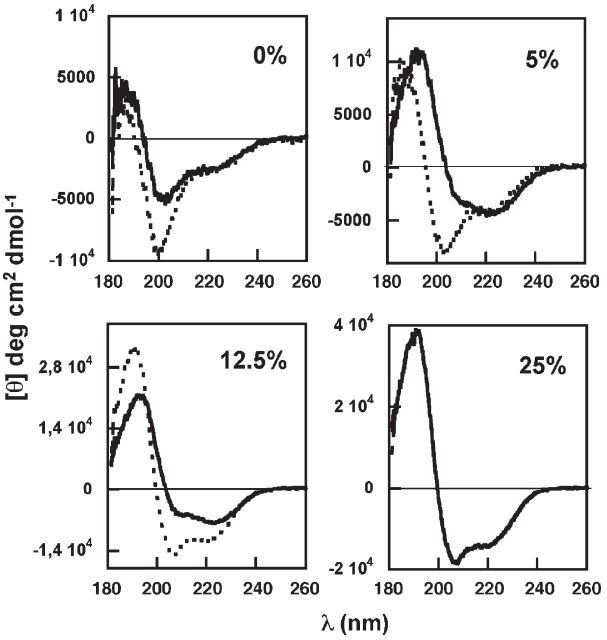

Figure 3. Assembly of FPK3 and 2F5ep sequences as determined by CD. Spectra of a FPK3:2F5ep mixture (1:1 molar ratio, continuous lines) with a varying amount of HFIP, as indicated in the panels. The dotted lines correspond to the spectra calculated by adding the individual FPK3 and 2F5ep signals. In 25% HFIP, both spectra are superimposed.

Table 2. Interactions of FPK3 with sequences bearing the 2F5 epitope as inferred from CD spectroscopic data

Peptide mixture (HFIP %)	$[\theta]_{222}/[\theta]_{208}$	
	Experimental	Calculated [b]
FPK3:2F5ep [a] (0)	0.62	0.46
FPK3:2F5ep (5)	1.53	0.63
FPK3:2F5ep (12.5)	1.34	0.78
FPK3:2F5ep (25)	0.76	0.78
FPK3:2F5preTM (0)	0.79	0.50
FPK3:2F5preTM (5)	1.12	0.75
FPK3:2F5preTM (10)	1.02	0.91
FPK3:2F5preTM (25)	0.84	0.83

[a] Equimolar mixtures.
[b] Spectra calculated as the sum of individual peptide signals.

mixture (Figure 4 and Table 3). Only the internal FP sequence representing the IFPK2 oligopeptide induced spectral differences that were qualitatively similar to those induced by the complete FP sequence (Figure 4(a)). In addition, experiments in which 2F5ep was titrated with increasing amounts of IFPK2 indicated that the oligopeptide-induced spectral changes saturate at approximately equimolar ratios (Figure 4(b)). In contrast, the amino-terminal (NFPK2) and carboxy-terminal (CFP) derivatives did not display any significant effects. Internal FP sequences scrambled following an ordered (Scr1IFPK2) or a disordered (Scr2IFPK2)

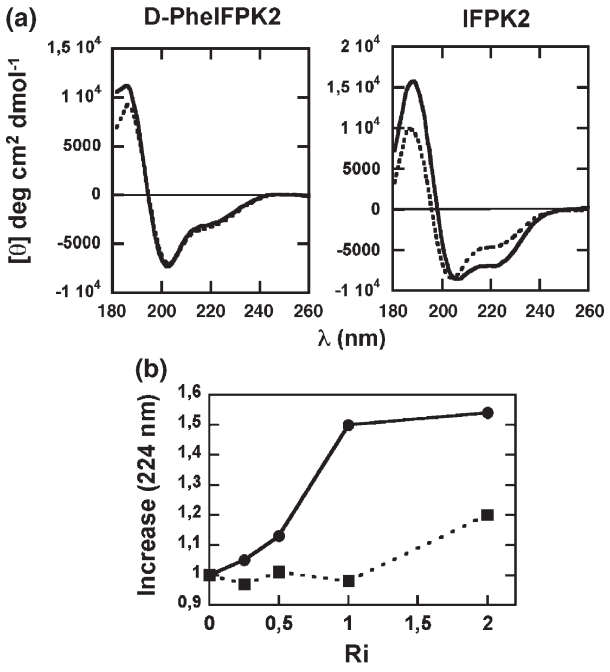

Figure 4. Specificity of FP-2F5ep interactions inferred using soluble short derivatives. (a) Spectra of IFPK2:2F5ep (right-hand panel) and D-PheIFPK2:2F5ep (left-hand panel) mixtures (1:1 molar ratios) in 5% HFIP. Continuous and dotted lines are as in the previous Figure. Sequences as given in Table 3. (b) Increase in absorption at 224 nm (experimental over calculated signal) as a function of the IFPK2:2F5ep (circles and continuous line) and D-PheIFPK2:2F5ep (squares and dotted line) molar ratios (*Ri*).

Table 3. Sequences of shorter soluble peptides used to assess the specificity of the FP–2F5ep interaction

Name	Sequence	Interaction [a]
IFPK2	LFLGFLGKK	+
NFPK2	AVGIGALKK	–
CFP	GAAGSTMGA	–
Scr1IFPK2	FFGGLLLKK	–
Scr2IFPK2	FGLLGFLKK	–
D-PheIFPK2	LfLGfLGKK	–

[a] As inferred from CD spectroscopic data (Figure 4).

pattern did not affect the structure of 2F5ep either. Moreover, D-PheIFPK2 did not cause the spectral differences observed in the presence of IFPK2 (Figure 4(a) and (b)). Within this derivative, both conserved L-Phe residues were substituted by the corresponding D-Phe stereoisomers. Thus, even though D-PheIFPK2 and IFPK2 sequences distributed hydrophobicity equally, it was expected that these peptides would display different steric constraints within a putative complex. The observation that D-PheIFPK2 did not affect the conformation of 2F5ep supports the existence of stereospecific interactions between IFPK2 and 2F5ep, and suggests structural grounds to explain the conservation of FLGFLG tripeptide duplication.[16]

The results displayed in Figure 5 indicate that the stereospecific 2F5ep–IFPK2 interactions had an effect also on epitope recognition by Mab2F5. Antibody affinity to the linear epitope and to IFPK2:2F5ep and D-PheIFPK2:2F5ep mixtures was inferred from the ability of the peptide to block antibody recognition of functional gp41 expressed on cell surfaces (Figure 5(a)). The IFPK2: 2F5ep mixture reverted the blockage of syncytium formation induced by Mab2F5 more efficiently than 2F5ep alone (Figure 5(b)). Dependency of inhibition on the molar ratio (Figure 5(c)) revealed a correlation between Mab2F5-2F5ep binding enhancement and stereospecific induction of structure by IFPK2 (Figure 4(b)). In contrast, the D-PheIFPK2 derivative had no effect on the inhibition exerted by 2F5ep (Figure 5(b) and (c)). These observations are consistent with the Mab2F5 binding surface being better mimicked within the 2F5ep structures that were induced specifically by the interaction with IFPK2.

When taken together, the results displayed in Figures 3–5 are consistent with the existence of FP-induced specific conformational effects on the 2F5ep region of gp41 in solution. The immunological studies described below further support the hypothesis that FP residues might be involved in the stabilization of the gp41 stem-like structures recognized by Mab2F5 (Figures 6–9). The membrane-proximal sequence selected as immunogen (represented by the peptide 2F5preTM) combined the 2F5 epitope and the highly aromatic preTM sequence previously shown to form homo-oligomers in solution (Table 1 and Figure 6(a)).[23] Accordingly, preTM homodimers and homotrimers could be observed in 5 μM and in

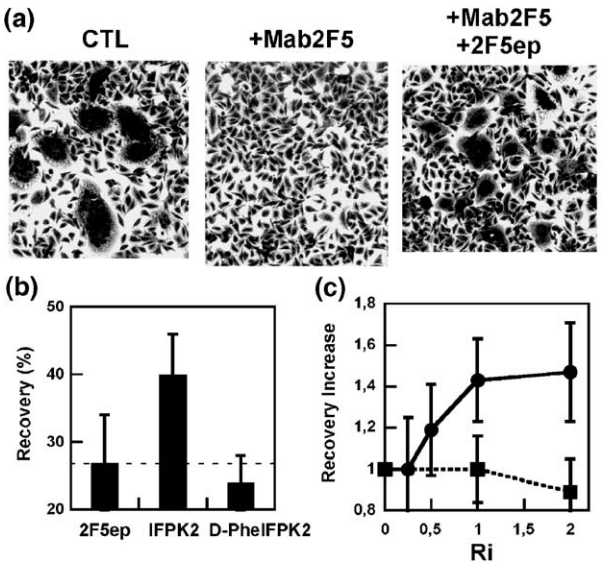

Figure 5. IFP-induced structure-specific enhancement of epitope recognition by Mab2F5. (a) Mab2F5-2F5ep binding was inferred from the recovery of gp41 fusion activity by pre-incubation of Mab2F5 with peptides (i.e. inhibition of Mab2F5-gp41 binding). CTL, untreated control (100% Mab2F5-gp41 binding inhibition); +Mab2F5, cells treated with Mab2F5 alone (5 μg/well, 0% Mab2F5-gp41 binding inhibition); +Mab2F5/+2F5ep, Mab was pre-incubated with 2F5ep (1.2 μM) before addition to the cells. (b) Percentage of fusion recovery by pre-incubation with 2F5ep (1.2 μM) or IFPK2:2F5ep and D-PheIFPK2:2F5ep mixtures (2:1 molar ratio). The value of 100% recovery was established as the number of nuclei present in syncytial plaques (fused cells containing more than four nuclei) per field in CTL samples (b). (c) Fusion recovery increase (mixture over peptide-alone value) as a function of the IFPK2:2F5ep (circles and continuous line) and D-PheIFPK2:2F5ep (squares and dotted line) molar ratios (*Ri*). Fixed 2F5ep concentration was 1.2 μM. Plotted values in (b) and (c) represent the means plus standard deviations of four independent experiments.

10 μM bis[sulfosuccinimidyl]suberate (BS^3) (Figure 6(b), left panel, lanes 2 and 3). Homodimers were also prominent at a concentration of BS^3 of 20 μM, conditions permissive to extensive preTM cross-linking (Figure 6(b), left panel, lane 4). PreTM homo-oligomerization was attenuated within longer 2F5preTM peptides (lane 2 in the right-hand panel of Figure 6(b)). However, incubation of 2F5preTM with FPK3 promoted the process (lane 3), suggesting that interactions between 2F5ep and FP residues might also stabilize oligomeric complexes in this case.

CD analyses offered further support for the existence of FPK3–2F5preTM interactions within the oligomeric complexes (Figure 6(c)). As compared with the spectrum calculated for non-interacting sequences (dotted line), the experimentally measured FPK3:2F5preTM mixture spectrum in buffer (continuous line) displayed weaker but defined negative bands at ca 208 nm and 222 nm, and positive absorption at 192 nm (Figure 6(c), left-hand panel). In addition, the experimental mixture spectrum, but not the spectrum calculated for non-interacting sequences, displayed an $[\theta]_{222}/[\theta]_{208}$ ellipticity ratio >1 in 5% HFIP (Figure 6(c), right-hand panel, and see Table 2).

The data shown in Figure 7 suggest that the interactions established between FP residues and 2F5preTM were also structure-specific. As evidenced by the cross-linking experiments, IFPK2, but not D-PheIFPK2 or Scr2IFPK2, sustained 2F5preTM homo-oligomerization (Figure 7(a)). Similarly, calculated (dotted line) and measured (continuous line) CD spectra displayed in Figure 7(b) differed in the case of IFPK2:2F5preTM mixtures (right-hand panel), but were superimposed in the case of D-PheIFPK2:2F5-preTM mixtures (left-hand panel). Thus, according to the oligomerization and CD data, FP residues

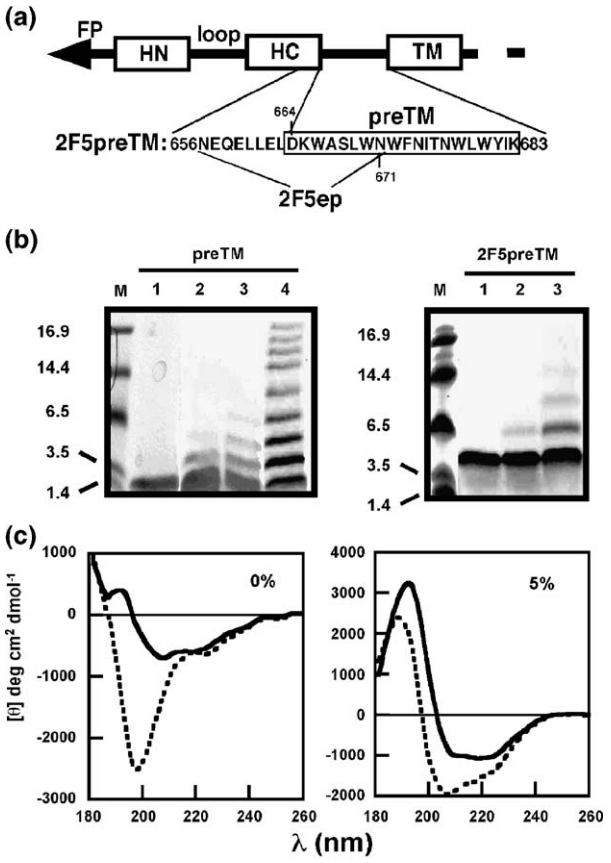

Figure 6. Membrane-proximal gp41 sequence used for immunization assays and its assembly with FPK3 in solution. (a) A representation of gp41 and the designation of 2F5preTM. (b) Self-association of the gp41 preTM (left-hand panel) and 2F5preTM (right-hand panel) sequences in solution. PreTM was incubated alone (lane 1) or in presence of 5 μM, 10 μM or 20 μM BS^3 for 30 minutes (lanes 2–4). 2F5preTM was incubated alone (lane 1) or in the presence of 20 μM BS^3 (lanes 2 and 3). The sample in lane 3 was pre-mixed with FPK3 at a 1:1 molar ratio. Molecular mass (kDa) markers were run as indicated. (c) FPK3-2F5preTM assembly as determined by CD. Measured (continuous line) and calculated (dotted line) CD spectra of the FPK3:2F5preTM mixture (1:1 molar ratio). The amount of HFIP is indicated.

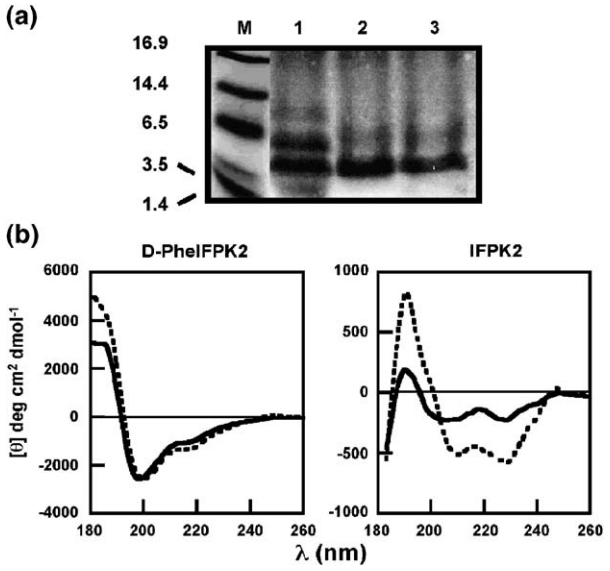

Figure 7. Specificity of FP-2F5preTM interactions inferred using soluble short derivatives. (a) Self-association of 2F5preTM pre-mixed with IFPK2 (lane 1), D-PheIFPK2 (lane 2) or Scr2IFPK2 (lane 3). Mixtures (nonapeptide/2F5preTM, 3:1 molar ratio) were incubated in presence of 1.5 mM BS^3 for 30 min. Molecular mass (kDa) markers were run as indicated. (b) Spectra of IFPK2:2F5preTM (right-hand panel) and D-PheIFPK2:2-F5ep (left-hand panel) mixtures (2:1 molar ratios) in 5% HFIP. Continuous and dotted lines are as in Figure 6.

appear to induce the adoption of specific structures by the 2F5preTM sequence.

In line with the existence of structure-specific effects, the results displayed in Figure 8 confirm that the FPK3-2F5preTM interactions also enhanced Mab2F5 recognition. Both 2F5preTM and the FPK3:2F5preTM mixture reversed the blockage of syncytium formation induced by Mab2F5. However, quantification of this inhibitory effect as a function of peptide concentration (Figure 7(b)) revealed $K_{d(appar)}$ values of 0.36(±0.15) μM and 0.82(±0.42) μM for the mixture (continuous trace) and the 2F5preTM (dotted trace), respectively. The lower dissociation constant suggests that the Mab2F5 antigen was better mimicked by the FP-stabilized complex.

In summary, the results displayed in Figures 6–8 suggest the existence of an oligomeric FPK3–2F5preTM complex in solution, whose conformation is defined by the interaction between both sequences. Figure 9 illustrates the results of experiments performed to compare this complex and the linear 2F5preTM peptide in their ability to induce immune responses in rabbits. The sera of rabbits immunized with 2F5preTM (''linear'') contained anti-2F5preTM and anti-2F5ep antibodies, but hardly any anti-preTM antibodies (Figure 9(a), left-hand panel). A similar response was observed in rabbits immunized with the FPK3:2F5preTM mixture (''mixture'') in alum (center panel). Given that lowering the polarity of the medium induced complex dissociation (Table 2), we also analyzed the immunogenicity of the mixture presented in water-in-oil emulsions (Freund's adjuvant). Sera recovered from rabbits immunized with the FPK3:2F5preTM mixture in Freund's adjuvant (mixture (Freund)) were different (right-hand panel). They recognized 2F5preTM immobilized in plaques, but displayed a weaker affinity for 2F5ep or preTM.

Competitive ELISA demonstrated that only the IgGs recovered from ''mixture'' sera competed efficiently with Mab2F5 for epitope recognition in plaques (Figure 9(b)). These IgGs also interfered with Mab2F5-gp41 binding (Figure 9(c)), since cell-IgG pre-incubation blocked the capacity of Mab2F5 to inhibit fusion (filled bars). In comparison, IgGs from the immunization with the linear peptide and those generated with mixture (Freund) exerted no significant effect. Notably, the ''linear'' IgGs recognized in plaques a recombinant gp41 ectodomain lacking the FP (open bars) more efficiently than the mixture IgGs. In comparison, gp41 was poorly recognized by the mixture (Freund) IgGs under all conditions. In conjunction, these results are consistent with the presence of antibodies that bind a native 2F5 epitope in functional gp41 in the ''mixture'' IgGs, while those IgGs induced by the linear sequence did not recognize a similar structure.

Discussion

The two membrane-transferring regions that are folded as part of the protruding gp41 ectodomain seem to constitute a functional determinant.[15,23] Upon translocation, these regions are postulated to provoke the kind of membrane perturbations that ensure fusion-pore opening.[15,30–33] However, the organization of these hydrophobic sequences within the pre-fusion, metastable gp41 ectodomain remains unclear, which impairs our understanding of the mechanisms that drive the initial stages of fusion.

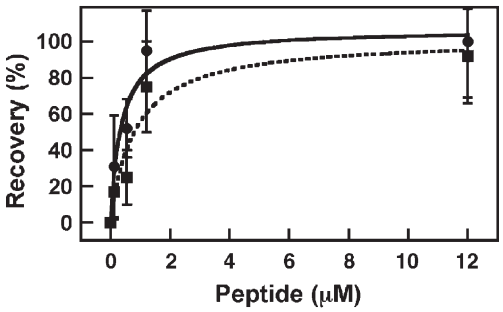

Figure 8. Inhibition of Mab2F5-gp41 binding by pre-incubation with 2F5preTM (squares and dotted line) or FPK3:2F5preTM mixture (1:1 molar ratio, circles and continuous line). The assay was calibrated as described in the legend to Figure 5. Plotted values represent the means plus standard deviations of four independent experiments. Half-maximal binding values ($K_{d(app)}$) were inferred by fitting the experimental values to hyperbolic functions and are given in the text (±standard errors).

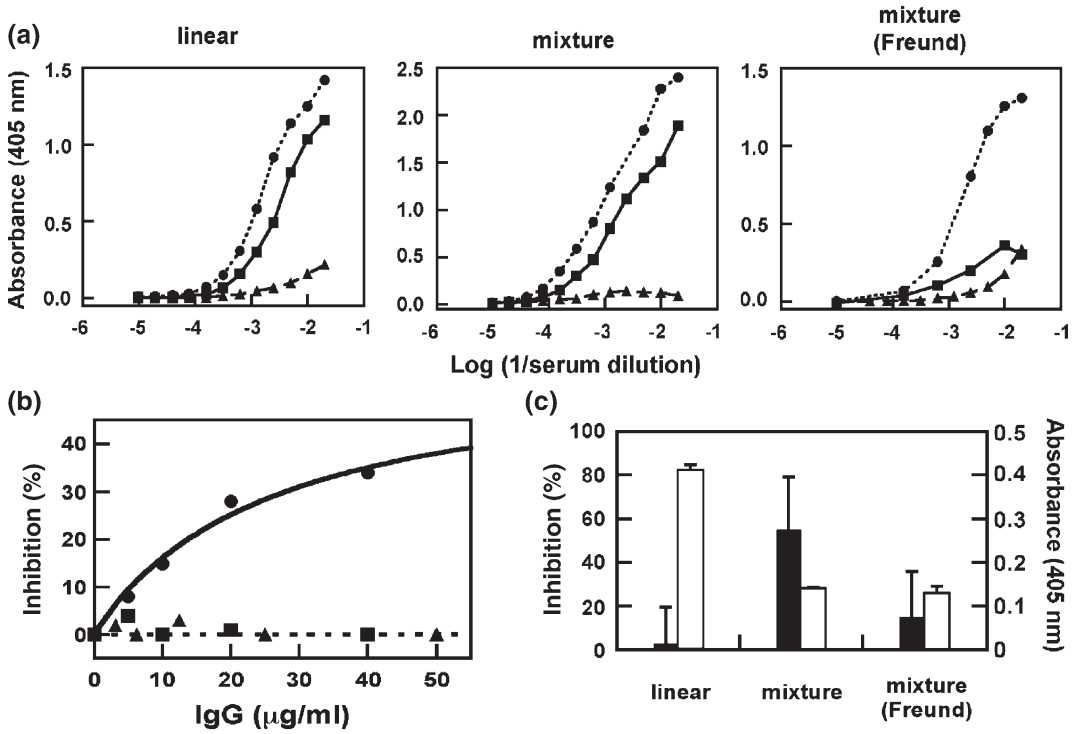

Figure 9. Immunogenicity of FPK3:2F5preTM mixtures and linear 2F5preTM peptide. (a) Sera obtained from rabbits immunized with 2F5preTM (linear) or FPK3:2F5preTM (mixture) in alum, or FPK3:2F5preTM (mixture (Freund)) in Freund's adjuvant, were titrated using 1.4 μM 2F5preTM (circles and dotted line), 2F5ep (squares and continuous lines) or preTM (triangles and broken line) immobilized in plaques. (b) Inhibition of Mab2F5-2F5ep binding by IgGs isolated from mixture (circles and continuous line), mixture-Freund (squares) and linear (triangles) sera. Comparable amounts of the linear and mixture IgGs bound to plaques were obtained by applying 2F5ep to the plaques at concentrations of 1 μg/ml and 2.5 μg/ml, respectively. (c) Inhibition of Mab2F5 (5 μg) binding to gp41 as inferred from the recovery of cell–cell fusion in syncytium assays (black bars) and recognition of gp41rec (1 μg) in ELISA plaques (white bars). Means plus standard deviation of three independent measurements are represented. In both assays 40 μg/ml of IgG were used.

Our results suggest that a carboxy-stem native structure recognized by Mab2F5 might be grafted into the amino-terminal FP. Indeed, the FP appears to be an element in gp41 that would be suitable to occlude the hydrophobic face of the epitope not bound by the antibody (Figures 1 and 2). The existence of specific tertiary interactions between these elements (Figures 3 and 4) relevant to the structure of gp41 stem (Figure 5) might well account for the high degree of conservation of FP residues such as the FLG tripeptide,[16] which cannot be explained by the simple hydrophobicity or amphipathicity necessary to produce membrane insertion.

Current knowledge on the conformation/orientation of the pre-fusion native states of membrane-proximal gp41 region derives from the peptide-epitope structures bound to antigen-binding antibody fragments 2F5 (Fab2F5) and 4E10 (Fab4E10).[22,34,35] Fab2F5 binds the gp41 657EQELLELDKWASLW670 sequence in an extended + turns non-helical conformation.[22] The 2F5 epitope-representing sequences have been shown to be structurally flexible, adopting several conformations in solution, including turns and 3_{10}-helical and α-helical structures.[25,36,37] When compared to the addition of CD signals arising from non-interacting FPK3 and 2F5ep, FPK3:2F5ep mixtures in buffer displayed weaker negative bands centered at ≈200–205 nm and positive absorption at 190 nm (Figure 3), which might denote a more populated type I β-turn conformer in the samples.[38,39] Nonetheless, an increase in β-type extended structures cannot be excluded, since small β-rich proteins may exhibit similar CD spectra.[40,41] In media with a low content of HFIP, CD changes were compatible with interacting helices.[27,28] However, similar spectra have been correlated with conformers containing a considerable type I β-turn population.[38,39] Thus, our CD results are compatible with the idea that specific interactions with FP might stabilize 2F5ep native-like conformations when co-assembled.

In contrast, Fab4E10 binds the sequence 670WNWFNITNW678 adjacent to 2F5 epitope adopting an almost fully helical structure,[34] a conformation that is stable also in membrane environments.[23,42,43] The Fab4E10-bound peptide structure also shows interdigitation of indole side-chains of two helices that interact through the faces not bound by the antibodies.[34] This fact would be consistent with our results showing that the preTM region may oligomerize in solution (Figure 6).[23] Also in accordance with this observation, FP promotes specifically the formation of oligomeric 2F5preTM complexes that are recognized by Mab2F5 with higher affinity than the peptide alone (Figures 6–8). We surmise that FP interactions might

impart specific conformations and orient the 2F5 epitope charged face towards the solvent, thereby reducing the electrostatic repulsion between amino-terminal acidic residues that might hinder self-association. The amphipathic complexes formed would emulate in solution a native structure of cognate gp41 (Figure 8) and retain the conformational constraints required to elicit in rabbits IgGs capable of interfering with Mab2F5-gp41 recognition (Figure 9).

The models displayed in Figure 10 illustrate that proposal. Packing of hydrophobic FP into an assembled FP–2F5preTM complex might sustain two effects (Figure 10(a)): (i) attainment by the linear 2F5 epitope stretch of a native-like orientation-conformation; and (ii) self-association of the aromatic-rich preTM domain. A similar structural organization might also sustain the folding of membrane-partitioning elements within the globular gp41 ectodomain (Figure 10(b)). In support of this model, epitope-mapping studies have shown that Mab 25C2 (mapping amino acid residues 526 to 543) is able to block binding of Mabs interacting with both amino-terminal (D40) and membrane-proximal (T3) gp41 determinants.[19] In addition, early structural models proposed that the FP position relative to membrane-proximal sequences in the pre-fusion gp41 ectodomain were reminiscent of that found in the influenza fusogenic subunit.[18] This proposal was based on pioneering structural work by Wiley and co-workers, showing that conserved FP tucked into a pocket apposing carboxy-terminal sequences in the native pre-fusion HA2 ectodomain.[44] Thus, besides the compact six-helix bundles as fusion promoters,[3,44] class I fusion proteins might utilize similar motifs to hide and control the membrane-active sequences within metastable structures.

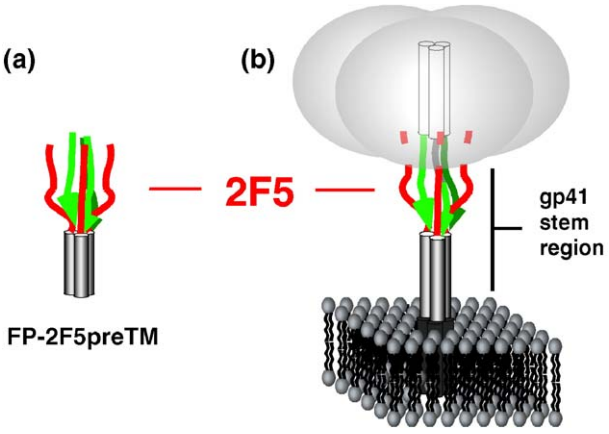

Figure 10. (a) Putative arrangement of the FP-2F5preTM complex and (b) a schematic model for its organization within extraviral gp41 stem region. Amino-terminal FP (green arrow) would interact with 2F5 continuous epitope region and stabilize native-like structures (red line). PreTM domain (light gray cylinders) would self-assemble into trimers. In the Env complex, this region is followed by the transmembrane domain (dark gray cylinders). Preceding the FP region, a trimeric coiled-coil HN region (white cylinders) might exist occluded by surface gp120 subunit (transparent spheres).

Mab2F5 recognizes poorly characterized pre-fusion native structures, as well as fusion-intermediate forms of gp41.[45–47] Therefore, the model in Figure 10(b) might represent the native gp41 ectodomain structure predominant in the virion Env complex, or else an intermediate in the fusion pathway trapped by the FP interaction. Conversely, Mab2F5 reactivity is inhibited by six-helix bundle formation, indicating that the epitope is occluded within the low-energy gp41 structure.[48] Thus, our data in Figures 6–9 would support the formation of an FP-2F5preTM complex that might occur before FP insertion into membranes and six-helix bundle formation. A docking surface for neutralizing antibodies that recognize gp41 might assemble within such a complex. This raises the possibility that recreating FP-induced interaction structures might be important to the design of effective synthetic AIDS vaccines.

Materials and Methods

Materials

The sequences displayed in Tables 1 and 3 were synthesized in C-terminal carboxamide form by solid phase methods using Fmoc chemistry, purified to near homogeneity by HPLC and characterized by MALDI-TOF mass spectrometry. Overlapping HIV-1 consensus subtype B Env (15-mer) peptides 8886 to 8898 and 8925 to 8927 were obtained from the NIH AIDS Research and Reference Reagent Program (contributed by Anaspec, Inc.). Peptide stock solutions were prepared in dimethyl sulfoxide (DMSO: spectroscopy grade) and the concentrations determined by the bicinchoninic acid microassay (Pierce, Rockford, IL, USA). Recombinant gp41 from HXB2 molecular clone (*Env* amino acid residues 546–682, i.e. the gp41 ectodomain in the absence of the FP sequence) expressed in *Pichia pastoris* was obtained from the EU Programme EVA/MRC Centralized Facility for AIDS Reagents, NIBSC, UK (grant number QLK2-CT-1999-00609 and GP828102). Mab2F5 was kindly donated by H. Katinger (Polymun Inc., Vienna, Austria).

ELISAs

Antibody specificity was determined by standard enzyme-linked immunosorbent assay (ELISA). Synthetic peptides (alone or mixed as complexes pre-formed in DMSO) and gp41rec were dissolved in phosphate-buffered saline (PBS) and immobilized overnight in C96 Maxisorp microplate wells (Nunc, Denmark). The degree of Mab binding was revealed through detection with alkaline phosphatase-conjugated goat immunoglobulin (Pierce, Rockford, IL, USA). Color was developed subsequently with the substrate *p*-nitrophenyl phosphate (Sigma, St. Louis, MO, USA), and absorbance at 405 nm was measured with a Synergy HT microplate reader (Bio-TEK Instruments Inc., VT, USA). Reactions were scored positive when absorbance was above the mean value plus three standard deviations of negative BSA controls. For competition ELISA, defined volumes of competing IgGs were pre-mixed with the Mab and added to the blocked wells.

Secondary structure determination

Circular dichroism (CD) measurements were carried out with a temperature-controlled Jasco J-810 CD spectropolarimeter calibrated routinely with (1S)-(+)-10-camphorsulfonic acid, ammonium salt. Peptide stock samples consisted of single sequences or mixtures preincubated in DMSO, lyophilized and finally dissolved at a concentration of 0.03 mM in 2 mM Hepes (pH 7.4). Spectra were measured in a 1 mm path-length quartz cell equilibrated initially at 25 °C. Data were taken with a 1 nm band-width, a speed of 20 nm/min, and the results of five scans were averaged.

Chemical cross-linking

Peptide homo-oligomerization was analyzed as described.[23] Samples consisted of 50 μg of peptide incubated in DMSO for 30 min before lyophilization. Lyophilized samples were resuspended in buffer and incubated in the presence or in the absence of the bifunctional cross-linking reagent BS^3 (Pierce) for 1 h at 37 °C. Cross-linked complexes were prepared for SDS-PAGE and resolved on Tris-tricine 16.5% (w/v) polyacrylamide gels. Gels were stained with Gelcode blue stain reagent (Pierce).

Blockade of syncytium inhibition

Syncytium formation assays were carried out using CHO-Env and HeLaT4$^+$ cells (ARRRP-NIH, contributed by C. Weiss and J. White, and by R. Axel, respectively). Fusion was inhibited by incubating Mab2F5 for 90 min with CHO-Env cells prior to co-culturing with HeLaT4$^+$ cells. The reversion of the inhibitory effect was achieved by incubating Mab2F5 with peptides for 90 min before adding it to the CHO-WT cells. In the case of the competition assay, IgGs and Mab2F5 were co-incubated with CHO-WT cells for 90 min before co-culturing with HeLaT4$^+$ cells.

Rabbit immunization

For immunization, 2F5preTM (linear) and FPK3:2F5preTM (1:1 molar ratio mixture) were prepared by dissolving them first in DMSO. After incubation for 15 min, the samples were lyophilized and subsequently reconstituted in 0.5 ml of PBS. Reconstituted samples were mixed with an equal volume of 1.3% (w/v) Alhydrogel (Superfos Biosector, Denmark) or Freund's adjuvant (Sigma). The IgGs were purified from the sera using protein-G-Sepharose HiTrap protein G HP columns (Amersham Biosciences Europe GmBh, Freiburg, Germany).

Acknowledgements

We are grateful to David Weliky for the initial supply of FPK3 and to Juan Asturias and Ignacio Ibarrola (Bial-Aristegi Inc., Bilbao, Spain) for technical assistance in rabbit immunization. We thank Nerea Huarte for her help with the experimental work. This study was supported by MCyT (EET 2001/1954, BMC 2003-01532) and the University of the Basque Country (042.310-13552/2001). M.L. was a recipient of a pre-doctoral fellowship of the Basque Government.

References

1. Wyatt, R. & Sodroski, J. (1998). The HIV-1 envelope glycoproteins: fusogens, antigens, and immunogens. *Science*, **280**, 1884–1888.
2. Doms, R. W. & Moore, J. P. (2000). HIV-1 membrane fusion: targets of opportunity. *J. Cell Biol.* **151**, F9–F14.
3. Eckert, D. M. & Kim, P. S. (2001). Mechanisms of viral fusion and its inhibition. *Annu. Rev. Biochem.* **70**, 777–810.
4. Gallo, S. A., Finnegan, C. M., Viard, M., Raviv, Y., Dimitrov, A., Rawat, S. S. *et al.* (2003). The HIV Env-mediated fusion. *Biochim. Biophys. Acta,* **1614**, 36–50.
5. Dalgleish, A. G., Beverley, P. C. L. & Clapham, P. R. (1984). The CD4 (T4) antigen is an essential component of the receptor for the AIDS retrovirus. *Nature*, **312**, 763–767.
6. Berger, E. A., Murphy, P. M. & Farber, J. M. (1999). Chemokine receptors as HIV-1 coreceptors: roles in viral entry, tropism, and disease. *Annu. Rev. Immunol.* **17**, 657–700.
7. Weissenhorn, W., Dessen, A., Harrison, S. C., Skehel, J. J. & Wiley, D. C. (1997). Atomic structure of the ectodomain from HIV-1 gp41. *Nature*, **387**, 426–428.
8. Chan, D. C., Fass, D., Berger, J. M. & Kim, P. S. (1997). Core structure of gp41 from the HIV-1 envelope glycoprotein. *Cell*, **89**, 263–273.
9. Furuta, R. A., Wild, C. T., Weng, Y. & Weiss, C. D. (1998). Capture of an early fusion-active conformation of HIV-1 gp41. *Nature Struct. Biol.* **5**, 276–279.
10. Muñoz-Barroso, I., Durell, S., Sakaguchi, K., Appella, E. & Blumenthal, R. (1998). Dilation of the human inmunodeficiency virus-1 envelope glycoprotein fusion pore revealed by the inhibitory action of a synthetic peptide from gp41. *J. Cell Biol.* **140**, 315–323.
11. Melikyan, G. B., Markosyan, R. M., Hemmati, H., Delmedico, M. K., Lambert, D. M. & Cohen, F. S. (2000). Evidence that the transition of HIV-1 gp41 into a six-helix bundle, not the bundle configuration, induces membrane fusion. *J. Cell Biol.* **151**, 413–423.
12. Freed, E. O., Myers, D. J. & Risser, R. (1990). Characterization of the fusion domain of the human immunodeficiency virus type 1 envelope glycoprotein gp41. *Proc. Natl Acad. Sci. USA,* **87**, 4650–4654.
13. Freed, E. O., Delwart, E. L., Buchschacher, G. L. & Panganiban, A. T. (1992). A mutation in the human immunodeficiency virus type 1 transmembrane glycoprotein gp41 dominantly interferes with fusion and infectivity. *Proc. Natl Acad. Sci. USA,* **89**, 70–74.
14. Salzwedel, K., West, J. & Hunter, E. (1999). A conserved tryptophan-rich motif in the membrane-proximal region of the human immunodeficiency virus type 1 gp41 ectodomain is important for env-mediated fusion and virus infectivity. *J. Virol.* **73**, 2469–2480.
15. Suárez, T., Gallaher, W. R., Agirre, A., Goñi, F. M. & Nieva, J. L. (2000). Membrane interface-interacting sequences within the ectodomain of the HIV-1 envelope glycoprotein: putative role during viral fusion. *J. Virol.* **74**, 8038–8047.
16. Gallaher, W. R. (1987). Detection of a fusion peptide

sequence in the transmembrane protein of the human immunodeficiency virus. *Cell*, **50**, 327–328.
17. Nieva, J. L. & Agirre, A. (2003). Are fusion peptides a good model to study viral cell fusion? *Biochim. Biophys. Acta,* **1614**, 104–115.
18. Gallaher, W. R., Ball, J. M., Garry, R. F., Griffin, M. C. & Montelaro, R. C. (1989). A general model for the transmembrane proteins of HIV and other retroviruses. *AIDS Res. Hum. Retroviruses,* **5**, 431–440.
19. Earl, P. L., Broder, C. C., Doms, R. W. & Moss, B. (1997). Epitope map of human immunodeficiency virus type 1 gp41 derived from 47 monoclonal antibodies produced by immunization with oligomeric envelope protein. *J. Virol.* **71**, 2674–2684.
20. Muster, T., Steindl, F., Purtscher, M., Trkola, A., Klima, A., Himmler, G. *et al.* (1993). A conserved neutralizing epitope on gp41 of human immunodeficiency virus type 1. *J. Virol.* **67**, 6642–6647.
21. Purtscher, M., Trkola, A., Gruber, G., Buchacher, A., Predl, R., Steindl, F. *et al.* (1994). A broadly neutralizing human monoclonal antibody against gp41 of human immunodeficiency virus type 1. *AIDS Res. Hum. Retroviruses,* **10**, 1651–1658.
22. Ofek, G., Tang, M., Sambor, A., Kainger, H., Mascola, J. R., Wyatt, R. & Kwong, P. D. (2004). Structure and mechanistic analysis of the anti-human immunodeficiency virus type 1 antibody 2F5 in complex with its gp41 epitope. *J. Virol.* **78**, 10724–10737.
23. Sáez-Cirión, A., Arrondo, J. L. R., Gómara, M. J., Lorizate, M., Iloro, I., Melikyan, G. & Nieva, J. L. (2003). Structural and functional roles of HIV-1 gp41 pre-transmembrane sequence segmentation. *Biophys. J.* **85**, 3769–3780.
24. Parker, C. E., Deterding, L. J., Hager-Braun, C., Binley, J. M., Schulke, N., Katinger, H. *et al.* (2001). Fine definition of the epitope on the gp41 glycoprotein of human immunodeficiency virus type 1 for the neutralizing monoclonal antibody 2F5. *J. Virol.* **75**, 10906–10911.
25. Barbato, G., Bianchi, E., Ingallinella, P., Hurni, W. H., Miller, M. D., Ciliberto, G. *et al.* (2003). Structural analysis of the epitope of the anti-HIV antibody 2F5 sheds light into its mechanism of neutralization and HIV fusion. *J. Mol. Biol.* **330**, 1101–1115.
26. Yang, R., Yang, J. & Weliky, D. P. (2003). Synthesis, enhanced fusogenicity, and solid state NMR measurements of cross-linked HIV-1 fusion peptides. *Biochemistry,* **42**, 3527–3535.
27. Keating, A. E., Malashkevich, V. N., Tidor, B. & Kim, P. S. (2001). Side-chain repacking calculations for predicting structures and stabilities of heterodimeric coiled coils. *Proc. Natl Acad. Sci. USA,* **98**, 14825–14830.
28. Litowski, J. R. & Hodges, R. S. (2002). Designing heterodimeric two-stranded alpha-helical coiled-coils. Effects of hydrophobicity and alpha-helical propensity on protein folding, stability, and specificity. *J. Biol. Chem.* **277**, 37272–37279.
29. Park, K., Perczel, A. & Fasman, G. D. (1992). Differentiation between transmembrane helices and peripheral helices by the deconvolution of circular dichroism spectra of membrane proteins. *Protein Sci.* **1**, 1032–1049.
30. Nieva, J. L., Nir, S., Muga, A., Goñi, F. M. & Wilschut, J. (1994). Interaction of the HIV-1 fusion peptide with phospholipid vesicles: different structural requirements for leakage and fusion. *Biochemistry,* **33**, 3201–3209.
31. Haque, M. E. & Lentz, B. R. (2002). Influence of gp41 fusion peptide on the kinetics of poly(ethylene glycol)-mediated model membrane fusion. *Biochemistry,* **41**, 10866–10876.
32. Sáez-Cirión, A., Nir, S., Lorizate, M., Agirre, A., Cruz, A., Pérez-Gil, J. & Nieva, J. L. (2002). Sphyngomyelin and cholesterol promote HIV-1 gp41 pretransmembrane sequence surface aggregation and membrane restructuring. *J. Biol. Chem.* **277**, 21776–21785.
33. Shnaper, S., Sackett, K., Gallo, S. A., Blumenthal, R. & Shai, Y. (2004). The C-and the N-terminal regions of glycoprotein 41 ectodomain fuse membranes enriched and not enriched with cholesterol, respectively. *J. Biol. Chem.* **279**, 18526–18534.
34. Cardoso, R. M., Zwick, M. B., Stanfield, R. L., Kunert, R., Binley, J. M., Katinger, H. *et al.* (2005). Broadly neutralizing anti-HIV antibody 4E10 recognizes a helical conformation of a highly conserved fusion-associated motif in gp41. *Immunity,* **22**, 163–173.
35. Zwick, M. B. (2005). The membrane-proximal external region of HIV-1 gp41: a vaccine target worth exploring. *AIDS*, **19**, 1725–1737.
36. Biron, Z., Khare, S., Samson, A. O., Hayek, Y., Naider, F. & Anglister, J. (2002). A monomeric 3(10)-helix is formed in water by a 13-residue peptide representing the neutralizing determinant of HIV-1 on gp41. *Biochemistry,* **41**, 12687–12696.
37. Joyce, J. G., Hurni, W. M., Bogusky, M. J., Garsky, V. M., Liang, X., Citron, M. P. *et al.* (2002). Enhancement of alpha-helicity in the HIV-1 inhibitory peptide DP178 leads to an increased affinity for human monoclonal antibody 2F5 but does not elicit neutralizing responses in vitro. Implications for vaccine design. *J. Biol. Chem.* **277**, 45811–45820.
38. Perczel, A. & Fasman, G. D. (1992). Quantitative analysis of cyclic beta-turn models. *Protein Sci.* **1**, 378–395.
39. Perczel, A. & Hollósi, M. (1996). Turns. In *Circular Dichroism and the Conformational Analysis of Biomolecules* (Fasman, G. D., ed), pp. 285–380, Plenum Press, New York.
40. Greenfield, N. J. (1996). Methods to estimate the conformation of proteins and polypeptides from circular dichroism data. *Anal. Biochem.* **235**, 1–10.
41. Sreerama, N. & Woody, R. W. (2004). Computation and analysis of protein circular dichroism spectra. *Method. Enzymol.* **383**, 318–351.
42. Suárez, T., Nir, S., Goñi, F. M., Saéz-Cirión, A. & Nieva, J. L. (2000). The pre-transmembrane region of the human immunodeficiency virus type-1 glycoprotein: a novel fusogenic sequence. *FEBS Letters*, **477**, 145–149.
43. Schibli, D. J., Montelaro, R. C. & Vogel, H. J. (2001). The membrane-proximal tryptophan-rich region of the HIV glycoprotein, gp41, forms a well-defined helix in dodecylphosphocholine micelles. *Biochemistry,* **40**, 9570–9578.
44. Skehel, J. J. & Wiley, D. C. (2000). Receptor binding and membrane fusion in virus entry: the influenza hemagglutinin. *Annu. Rev. Biochem.* **69**, 531–569.
45. Sattentau, Q. J., Zolla-Pazner, S. & Poignard, P. (1995). Epitope exposure on functional, oligomeric HIV-1 gp41 molecules. *Virology*, **206**, 713–717.
46. Finnegan, C. M., Berg, W., Lewis, G. K. & DeVico, A. L. (2002). ntigenic properties of the human immunodeficiency virus transmembrane glycoprotein during cell-cell fusion. *J. Virol.* **76**, 12123–12134.
47. De Rosny, E., Vassell, R., Jiang, S., Kunert, R. & Weiss, C. D. (2004). Binding of the 2F5 monoclonal antibody to native and fusion-intermediate forms of human

immunodeficiency virus type 1 gp41: implications for fusion-inducing conformational changes. *J. Virol.* **78**, 2627–2631.
48. Gorny, M. K. & Zolla-Pazner, S. (2000). Recognition by human monoclonal antibodies of free and complexed peptides representing the prefusogenic and fusogenic forms of human immunodeficiency virus type 1 gp41. *J. Virol.* **74**, 6186–6192.
49. Wimley, W. C. & White, S. H. (1996). Experimentally determined hydrophobicity scale for proteins at membrane interfaces. *Nature Struct. Biol.* **3**, 842–848.

Edited by G. von Heijne

(Received 24 January 2006; received in revised form 24 April 2006; accepted 25 April 2006)
Available online 11 May 2006